RELATIVE ESTIMATE OF ACCURACY IN ORBIT DETERMINATION FROM A SHORT TRACKLET

Alessandro Vananti, Thomas Schildknecht

Astronomical Institute, University of Bern, Sidlerstrasse 5, CH-3012 Bern, Switzerland,
alessandro.vananti@aiub.unibe.ch, thomas.schildknecht@aiub.unibe.ch

ABSTRACT

The Astronomical Institute of the University of Bern (AIUB) is conducting several search campaigns for orbital debris. The debris objects are discovered during systematic survey observations. In general only a short observation arc, or tracklet, is available for most of these objects. From this discovery tracklet a first orbit determination is computed in order to be able to find the object again in subsequent follow-up observations. The additional observations are used in the orbit improvement process to obtain accurate orbits to be included in a catalogue.
In this paper, the accuracy of the initial orbit determination is analyzed. This depends on a number of factors: tracklet length, number of observations, type of orbit, astrometric error, and observation geometry. The latter is characterized by both the position of the object along its orbit and the location of the observing station. Different positions involve different distances from the target object and a different observing angle with respect to its orbital plane and trajectory. The present analysis aims at optimizing the geometry of the discovery observations depending on the considered orbit.

1. INTRODUCTION

The Astronomical Institute of the University of Bern (AIUB) is conducting optical search campaigns for high altitude objects using the ESA Space Debris Telescope (ESASDT) on Tenerife on behalf of ESA. The aim of these campaigns is to improve the statistical information about the populations of objects in Geostationary Orbits (GEO) [1], Geostationary Transfer Orbits (GTO) [2], and Medium Earth Orbits (MEO) [3]. A large amount of faint and unknown objects, as well as a new population of objects with a very high area-to-mass ratio have been observed within these surveys [4]. In general only a short observation arc is available for most of these objects. These short arcs do not allow determining an accurate full six parameter orbit. Normally, circular orbits are determined instead. A circular orbit is a good approximation for GEO, but not for eccentric orbits like GTO. Possible concepts for a catalogue of objects were developed in the framework of ESA studies for a European Space Surveillance Network [5][6]. AIUB participated in these studies, where the work focused on the selection of optical detectors, the development of survey strategies for high-altitude orbits, and on the performance estimation. According to the developed concepts, to improve the quality of the determined orbits for newly discovered objects, follow-up observations are conducted. Since the discovery track of an object usually consists of a small number (two to ten) of observations and the track length is only a few minutes, follow-up observations are needed in order to get a longer observation arc. Follow-ups from several nights are needed if the orbit should be accurate enough to be included into a catalogue. Several studies have investigated the optimal sequence of follow-ups and the time intervals between subsequent observations to achieve the best orbit accuracy [7][8]. From the investigations it resulted that e.g. for GEO at least two follow-up tracks are necessary to recover a discovered object during the following night. The ideal time interval between the tracks was found to be one hour. This allows recovering the object with the small field of view (FOV) of 0.7” at the ESASDT. The geometry of the observation is relevant for the accuracy of the orbit determination. The geometric factors essentially comprise the distance from the station to the object and the angle between the line of sight and the trajectory of the object. In this work the dependence of the accuracy in the orbit determination on these parameters is investigated.

2. CIRCULAR ORBITS

To illustrate the importance of the observation geometry some preliminary results in the case of circular orbits are examined. The geometry considered in the analysis of the problem is illustrated in Figure 1. The orbit plane coincides with the Earth equatorial plane. The angle α describes the geocentric difference in right ascension of the object in the positions C and D. In the case of one station A the object can be observed at the zenith (position C) or later at the position D.

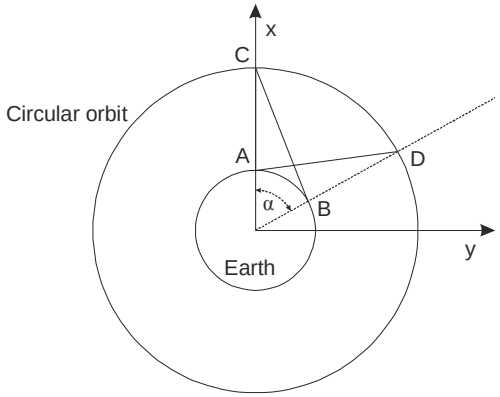

Figure 1. Geometry with circular orbit in the equatorial plane. The angle α indicates the difference in longitude or right ascension.

Simulations for GEO, MEO, and LEO orbits were performed with a mean astrometric error of 0.5” with tracklets consisting of three observations within 15 s. The initial orbit determination was calculated using the “Celmech” software environment developed at AIUB [9]. We analyse the degree of accuracy in the semimajor axis achieved in the orbit determination process. Figure 2 shows the formal error Δa in the semimajor axis as a function of the angle α for orbits in LEO, MEO, and GEO. The formal error is mainly dependent on two distinct components: the observation error and the length of the observed arc. There is obviously also a dependence from the number of observations, but we will not consider it in this study. In the observation error relevant for our considerations is the error Δα regarding the topocentric measured position in right ascension. The influence of Δα in the formal error Δa can be estimated using geometric considerations. Figure 3 shows for GEO the observation error $\Delta\alpha_{geo}$ at the geocenter as a function of the angle α for different error values Δα indicated in the color bar. The error at the geocenter is calculated propagating the measurement error Δα in the transformation formula from topocentric to geocentric coordinates. After this transformation the orbit determination in the simulations can be performed considering observations with error $\Delta\alpha_{geo}$ from a hypothetical station at the geocenter. In Figure 4 the error Δa as a function of the arc length is plotted for the three types of orbit. For more details on the results in this paragraph consult [10].

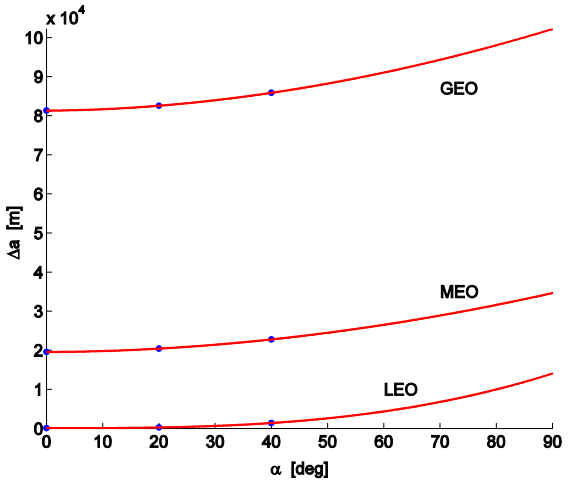

Figure 2. Formal error Δa in the semimajor axis as a function of α for LEO, MEO, and GEO orbits.

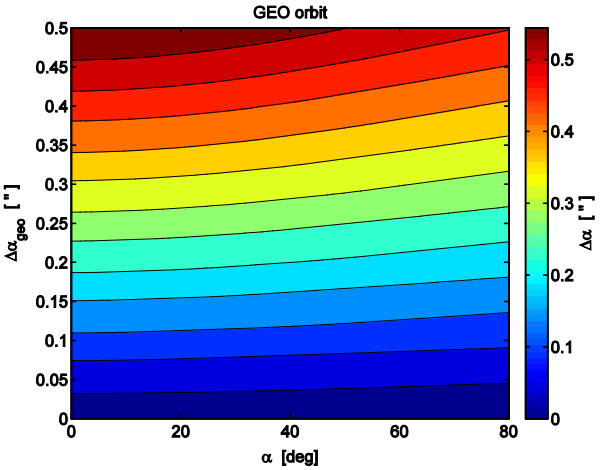

Figure 3. Error $\Delta\alpha_{geo}$ at the geocenter vs. angle α for different error values Δα for orbits in GEO.

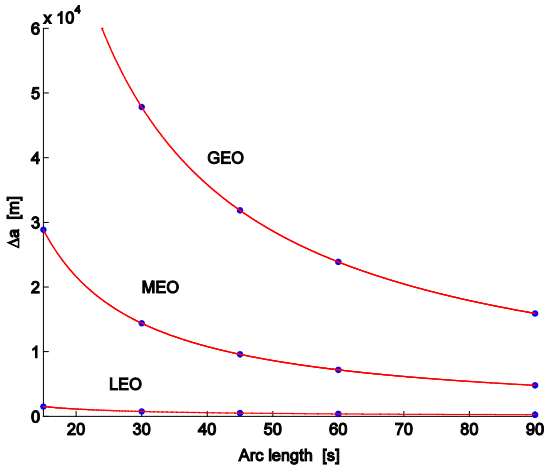

Figure 4. Formal error Δa as a function of the arc length with $\Delta\alpha_{geo}$ = 0.5” and three observations within the arc for LEO, MEO, and GEO orbits.

3. ELLIPTIC ORBITS

We want to extend the analysis to elliptic orbits. The goal is the relative estimate of the accuracy in the initial orbit determination. Thus not the absolute accuracy is estimated, only the relative accuracy variation as a function of the observer and object position. For this purpose a simplistic approach is used. For Keplerian orbits the following relations hold,

$$r(1+e\cos\theta) = a(1-e^2) \quad (1)$$

$$r^4\dot{\theta}^2 = \mu a(1-e^2) \quad (2)$$

where:
a = semimajor axis
e = eccentricity
r = geocentric radius to the orbiting object
Θ = true anomaly
μ = gravitational parameter

Inserting Eq. 1 into Eq. 2 eliminates the radius r:

$$a^3\dot{\theta}^2(1-e^2)^3 = \mu(1+e\cos\theta)^4 \quad (3)$$

The time derivative of Eq. 3 yields:

$$\ddot{\theta}(1+e\cos\theta) = -2e\dot{\theta}^2\sin\theta \quad (4)$$

From Eq. 4 it is possible to calculate the partial derivatives of e:

$$\frac{\partial e}{\partial\theta} = e^2\left(2\frac{\dot{\theta}^2}{\ddot{\theta}}\cos\theta - \sin\theta\right) \quad (5)$$

$$\frac{\partial e}{\partial\dot{\theta}} = \frac{4e^2\dot{\theta}}{\ddot{\theta}}\sin\theta \quad (6)$$

$$\frac{\partial e}{\partial\ddot{\theta}} = \frac{-2e^2\dot{\theta}^2}{\ddot{\theta}^2}\sin\theta \quad (7)$$

The partial derivatives of a can be calculated using the explicit derivatives of a,

$$\frac{\partial a}{\partial\theta} = \frac{-4ae\sin\theta}{3(1+e\cos\theta)} \quad (8)$$

$$\frac{\partial a}{\partial\dot{\theta}} = \frac{-2a}{3\dot{\theta}} \quad (9)$$

and the chain rule (e.g. w.r.t. Θ)

$$\frac{\partial a}{\partial\theta} = \frac{\partial a}{\partial e}\frac{\partial e}{\partial\theta} + \left.\frac{\partial a}{\partial\theta}\right|_e \quad (10)$$

with:

$$\frac{\partial a}{\partial e} = \frac{2a(2(1-e^2)\cos\theta + 3e(1+e\cos\theta))}{3(1+e\cos\theta)(1-e^2)} \quad (11)$$

The astrometric error is decomposed into a component in the orbital plane and perpendicular to it and transformed to errors at the geocenter as in the circular orbits case. Here, similarly to α we define the in-plane error $\Delta\Theta$ in the true anomaly and the error $\mathbf{\Delta n}$ in the vector $\mathbf{n}$ normal to the orbital plane. The transformation from the reference system I to the system embedded in the orbital plane R gives the partial derivatives for the inclination i and the ascending node Ω:

$$\left(\frac{\partial i}{\partial n_i}\right)_I = \sum_j R_{ij}\left(\frac{\partial i}{\partial n_j}\right)_R \quad (12)$$

$$\left(\frac{\partial \Omega}{\partial n_i}\right)_I = \sum_j R_{ij}\left(\frac{\partial \Omega}{\partial n_j}\right)_R \quad (13)$$

where R_{ij} is the rotation matrix based on the Euler angles, and n_i are the components of $\mathbf{n}$.

The total error Δa (similarly for e) is given by:

$$\Delta a^2 = \left(\frac{\partial a}{\partial\theta}\Delta\theta\right)^2 + \left(\frac{\partial a}{\partial\dot{\theta}}\Delta\dot{\theta}\right)^2 + \left(\frac{\partial a}{\partial\ddot{\theta}}\Delta\ddot{\theta}\right)^2 \quad (14)$$

where $\Delta\dot{\theta} \approx \frac{\Delta\theta}{\Delta t}$ and $\Delta\ddot{\theta} \approx \frac{\Delta\theta}{\Delta t^2}$.

With the above definition of $\Delta\ddot{\theta}$ the error in the semimajor axis tends to be overestimated. This reflects the worst case, where the computation of the orbit is based on angular accelerations. Other methods can determine the orbit more efficiently using velocity differences. Hence, to represent those methods in the later simulations the error Δa is calculated only up to the first time derivative term.
In analogous way for Δi (similarly for Ω):

$$\Delta i^2 = \left(\frac{\partial i}{\partial n_1}\Delta n_1\right)^2 + \left(\frac{\partial i}{\partial n_2}\Delta n_2\right)^2 \quad (15)$$

4. SIMULATIONS

In the following diagrams the estimated error is calculated using Eq. 14 and Eq. 15 for a given orbit as a function of the true anomaly Θ of the observed object and of the longitude λ of the observer, assuming the prime meridian parallel to the vernal point and latitude ϕ = 0°. The considered orbit has a = 42'000 km, $i = \Omega = \omega$ = 0°, and e = 0.1 or e = 0.5. The assumed astrometric error is 0.5'' and the tracklet length Δt = 15 s.

Figure 5 and Figure 6 show the relative error in the semimajor axis with e = 0.1 and e= 0.5 respectively, while Figure 7 and Figure 8 illustrate the dependency related to the eccentricity. The triangle regions in dark blue indicate that the object is not visible. From the diagrams it turns out that the semimajor axis can be better determined close to the perigee. This is probably due to the fact that, keeping a constant tracklet time interval, the arc covered is the longest at the perigee. The situation is accentuated with a bigger eccentricity. On the other hand the eccentricity is bad determined at perigee and apogee, where the angular acceleration is the smallest. If the eccentricity of the orbit is increased the region with higher accuracy is shifted towards smaller values of the true anomaly.

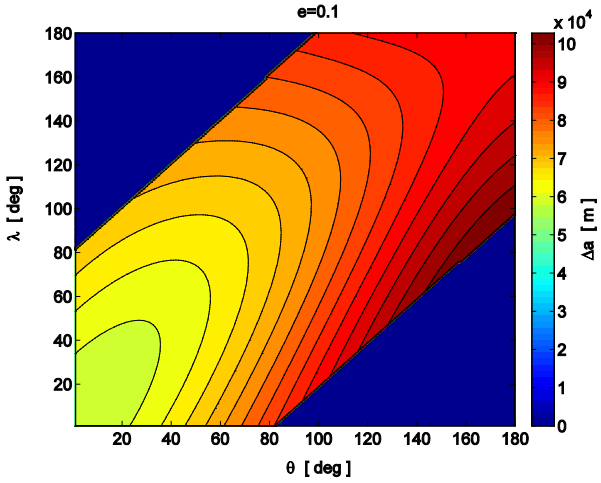

Figure 5. Relative error of semimajor axis Δa with eccentricity e = 0.1 as a function of true anomaly Θ and longitude λ.

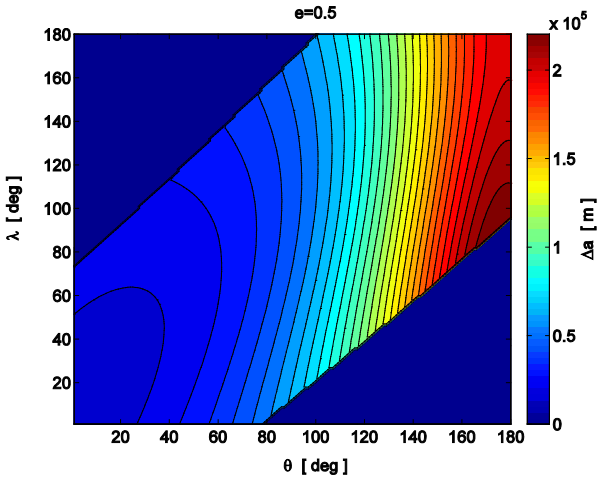

Figure 6. Relative error of semimajor axis Δa with eccentricity e = 0.5 as a function of true anomaly Θ and longitude λ.

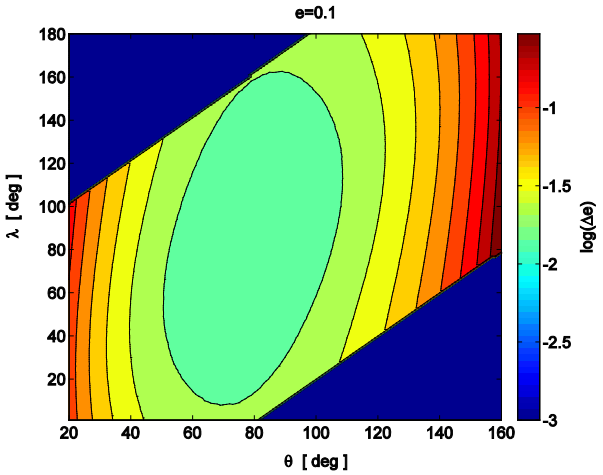

Figure 7. Relative error of eccentricity Δe with eccentricity e = 0.1 as a function of true anomaly Θ and longitude λ.

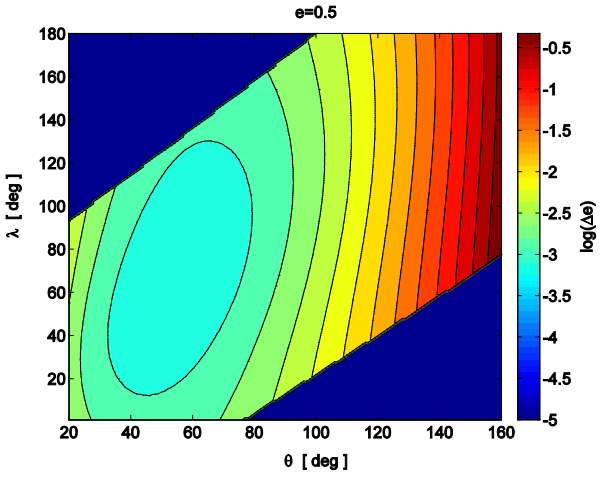

Figure 8. Relative error of eccentricity Δe with eccentricity e = 0.5 as a function of true anomaly Θ and longitude λ.

In Figure 9 and Figure 10 the error variation in the inclination with e = 0.1 and e= 0.5 are indicated. Figure 11 and Figure 12 exhibit the diagrams concerning the ascending node error. The minimal error in inclination is around 90° true anomaly. In this region the maximal elevation w.r.t. the equatorial plane is reached, which translates into a better accuracy of the plane definition. With higher eccentricity the error strongly increases in the non-optimal region around the apogee. The right ascension of the ascending node is better determined close to the node itself. For higher eccentricities the region with the maximal error is shifted towards bigger values of true anomaly.

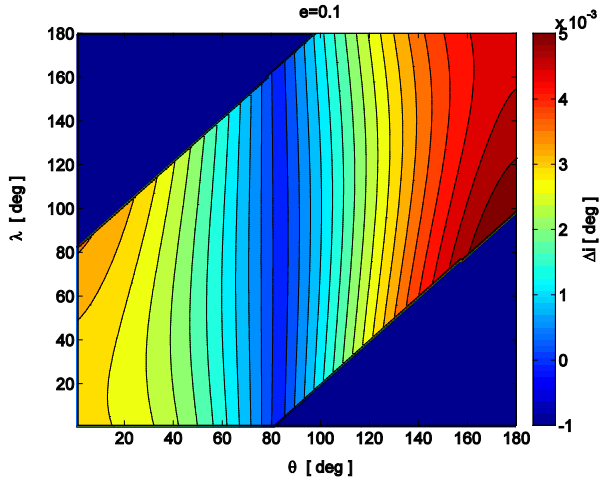

Figure 9. Relative error of inclination Δ*i* with eccentricity *e* = 0.1 as a function of true anomaly Θ and longitude λ.

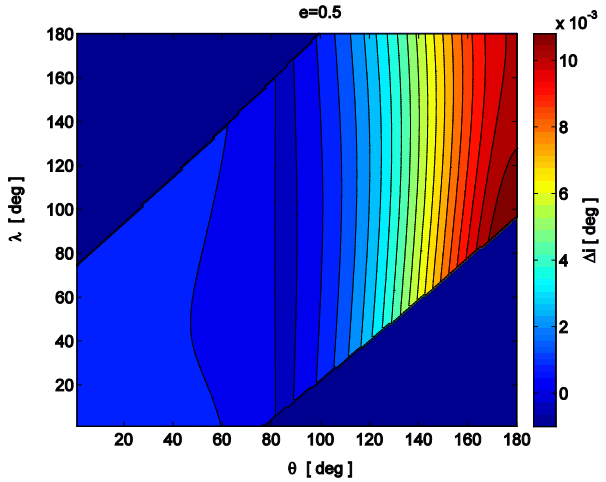

Figure 10. Relative error of inclination Δ*i* with eccentricity *e* = 0.5 as a function of true anomaly Θ and longitude λ

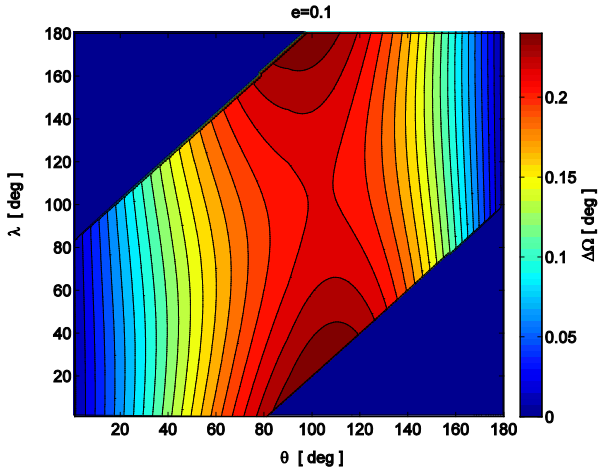

Figure 11. Relative error of ascending node ΔΩ with eccentricity *e* = 0.1 as a function of true anomaly Θ and longitude λ.

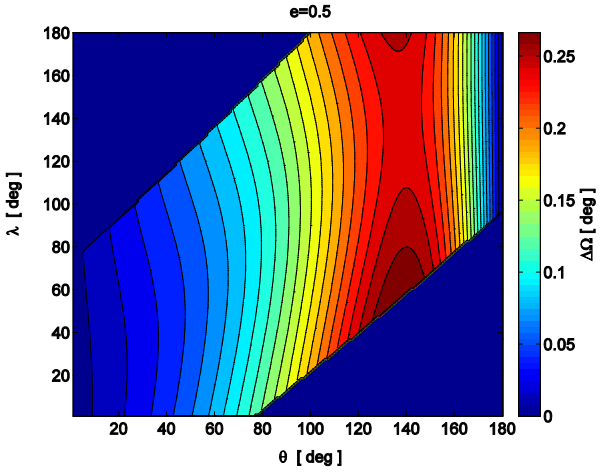

Figure 12. Relative error of ascending node ΔΩ with eccentricity *e* = 0.5 as a function of true anomaly Θ and longitude λ.

5. CONCLUSIONS

For the examined situations the considered errors in the orbital parameters are given by contributions according to the position of the object relative to the observer and the length of the observed arc. The contribution to the astrometric accuracy regarding the relative position can be calculated from the topocentric errors reduced to errors at the geocenter and the influence of arc length can be evaluated in the geocentric geometry. The error in the orbital parameters *a*, *e*, *i*, Ω for a given observation error and arc length can be estimated using a simple Keplerian model, where the error in the angular velocity and angular acceleration is given by the angular position error and the tracklet time interval. The total error is calculated through error propagation of angular position (for *I* and Ω), or also velocity, and acceleration (for *a* and *e*). Still, only the relative estimate of the error can be determined and not absolute values because the

approximation for the angular velocity and acceleration error is simplistic. Also for this reason not all derivative terms are considered, depending on the estimated orbital parameter.

Simulations were conducted for an elliptic orbit varying true anomaly of the object and longitude of the observer on the Equator. The results of the simulations can be easily interpreted with geometric considerations. The semimajor axis can be better determined close to the perigee where the arc is longest. The eccentricity is bad determined at perigee and apogee, where the angular acceleration is smallest. The minimal error in inclination occurs in the region where the maximal elevation w.r.t. the equatorial plane is reached, while the position of the ascending node is better determined close to the node itself.

The illustrated method serves as a quick way to estimate under which observation conditions the error in the orbit determination can be minimized, given an orbit and the observing station. Error maps similar to the ones shown above can be easily simulated with other variables or other orbits using the presented formalism.

6. REFERENCES

1. Schildknecht, T., R. Musci, M. Ploner, G. Beutler, W. Flury, J. Kuusela, J. de Leon Cruz, L. de Fatima Dominguez Palmero, Optical observations of space debris in GEO and in highly-eccentric orbits, *Advances in Space Research*, 34, 2004
2. Schildknecht, T., T. Flohrer, R. Musci, R. Jehn, Statistical analysis of the ESA optical space debris surveys, *Acta Astronautica*, 63, 2008
3. Hinze, A., T. Schildknecht, A. Vananti, H. Krag, Results from first space debris survey observations in MEO, *Proceedings of European Space Surveillance Conference*, Madrid, Spain, 2011
4. Musci, R., T. Schildknecht, M. Ploner, Analyzing long observation arcs for objects with high area-to-mass ratios in geostationary orbits, *Acta Astronautica*, 66, 2010
5. Flohrer, T., T. Schildknecht, R. Musci, E. Stöveken, Performance estimation for GEO space surveillance, *Advances in Space Research*, 35, 2005
6. Flohrer, T., T. Schildknecht, R. Musci, Proposed strategies for optical observations in a future European Space Surveillance network, *Advances in Space Research*, 41, 2008
7. Musci, R., T. Schildknecht, M. Ploner, Orbit improvement for GEO objects using follow-up observations, *Advances in Space Research*, 34, 2004
8. Musci, R., T. Schildknecht, M. Ploner, G. Beutler, Orbit improvement for GTO objects using follow-up observations, *Advances in Space Research*, 35, 2005
9. Beutler, G., *Methods of Celestial Mechanics*, Springer, Berlin, 2004
10. Vananti, A., T. Schildknecht, Dependence of Orbit Determination Accuracy on the Observer Position, *Proceedings of 6th European Conference on Space Debris*, Darmstadt, Germany, 2013